J Fluoresc (2015) 25:1537–1542
DOI 10.1007/s10895-015-1647-5

ORIGINAL ARTICLE

A New Fluorescent "Off-On" Sensor for Al^{3+} Derived from L-alanine and Salicylaldehyde

Smita Sarma [1] · Pradip Kr. Bhattacharyya [2] · Diganta Kumar Das [1]

Received: 20 May 2015 / Accepted: 18 August 2015 / Published online: 27 August 2015

Abstract The condensation product of L-alanine and salicylaldehyde was synthesised and characterised which was found to be selective fluorescent "on" sensor for Al^{3+} ion with the detection limit 10^{-6} M. The sensor is free of interferences from metal ions - Na^{+}, K^{+}, Ca^{2+}, Mn^{2+}, Co^{2+}, Ni^{2+}, Cu^{2+}, Pb^{2+}, Cd^{2+}, Hg^{2+} and Fe^{3+}. The Fluorescence and the UV/visible spectral data reveals a 1:1 interaction between the sensor and Al^{3+} ion with binding constant $10^{4.5}$. The DFT and TDDFT calculations confirm the structures of the sensor and the sensor-Al^{3+} complex.

Keywords Fluorescence · Sensor · Aluminium · L-alanine · Salicylaldehyde · TDDFT

Introduction

Aluminium (Al) is the most abundant metal in the earth's crust which is approximately 8 % of the total mass of the earth [1]. Modern life is largely dependent on Al in various forms like - light alloys, pharmaceuticals, water purification instruments, house hold utensils etc. [2] Al as such is normally not harmful but due to the environmental acidification the amount of harmful free Al^{3+} ions in soil increases. [3] These ions may reach human body through plants and may cause Alzheimer's disease, Parkinsonism dementia, osteoporosis, colic, and rickets. The Al^{3+} ions also damages plant roots [4]. The World Health Organization (WHO) listed Al^{3+} as one of the prime food pollutants and limited its concentration to 200 μg L^{-1} (7.41 μM) in drinking water [5]. WHO recommended tolerable weekly dietary human intake of Al^{3+} is 7.0 mg kg^{-1} body weight [6].Therefore the detection of Al^{3+} in water is of environmental, biological and human health importance. At present, different detection methods, like atomic absorption and emission, spectrophotometry, electrochemiluminscence and electrochemical methods are known for detection of Al^{3+} ion [7–10]. But due to the expensive instrumentations, requirement of highly-trained operators and complicated pretreatment makes these methods difficult for routine monitoring and applications.

Recently fluorescent sensors have gained considerable attention due to their operational simplicity, low detection limit, real-time detection and portability. A number of fluorescent sensors for determination of Al^{3+} have been reported in recent past. Fluorescent turn "on" Al^{3+}-sensor has been synthesized from 8-hydroxyquinoline-7-carbaldehyde and 4-aminopyrine [11]. Another turn "on" fluorescent sensor has been reported based on quinoline-coumarine [12]. A perylene tetracarboxylic bisimide based sensor reported to show green fluorescence under UV radiation [13]. Blue fluorescence enhancement for Al^{3+} was shown by Schiff base receptor, 1-((E)-(1,3-dihydroxy-2-(hydroxymethyl)propan-2-ylimino)methyl) naphthalene-2-ol [14]. A coumarin based Al^{3+} ion sensor is reported to act as turn "on" fluorescent Al^{3+} sensor by emitting bright blue fluorescence under UV radiation [15]. A dual fluorescent turn "off" and colorimetric sensor which shows a large red shift in fluorescent emission upon interaction with Al^{3+} is also reported [16]. They are attractive, although most of these sensors for Al^{3+} involve complicated synthetic procedure. Simple Schiff's bases as

✉ Diganta Kumar Das
digkdas@yahoo.com

[1] Department of Chemistry, Gauhati University, Guwahati, Assam 781 014, India

[2] Department of Chemistry, Arya Vidyapeeth College, Guwahati, Assam 781 016, India

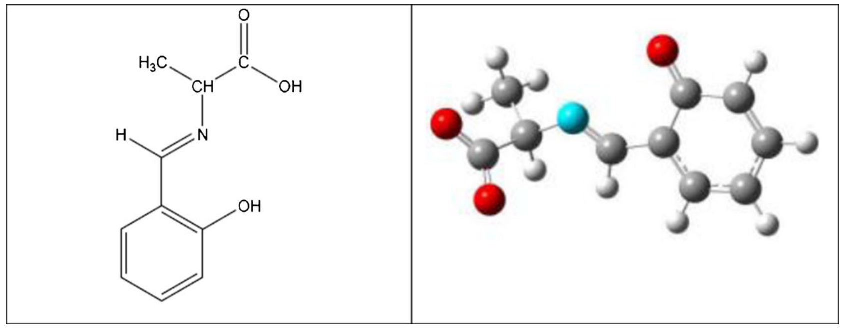

Scheme 1 Structure of **L** (*left*) and DFT optimised structure of **L** (*right*)

metal ion fluorescent sensors have attracted recent interest due to their simple synthetic procedure [17–20]. Therefore reporting of new fluorescent sensor which is of 'easy to synthesize' type, for Al^{3+} is fascinating and significant.

In recent years the DFT (density functional theory) methods have proven their wide range of applicability to ascertain structures of molecular complexes while the TDDFT (time dependent DFT) methods are successful in explaining the electronic properties [21–23].

In this paper we report a new "off-on" fluorescent sensor for Al^{3+} ion derived from L-alanine and salicylaldehyde which is selective for Al^{3+} over - Na^{+}, K^{+}, Ca^{2+}, Mn^{2+}, Co^{2+}, Ni^{2+}, Cu^{2+}, Pb^{2+}, Cd^{2+}, Hg^{2+} and Fe^{3+}. The DFT and the TDDFT calculations for the sensor and its interaction with Al^{3+} ion have also been reported.

Experimental

Chemicals and Experimental Techniques

All the chemicals (analytical grade) were from Loba Chemie except Methanol (Merck). The Metal salts were sulphates except $Pb(NO_3)_2$, $CaCl_2$, and $HgCl_2$. The Water used was double distilled in quartz distillation plant. The metal salts were recrystallised from water before use.

The Fluorescence spectra measurements were performed in a Hitachi FL-2500 florescence spectrophotometer, using a quartz cuvette (1 cm), and both the excitation and emission band passes were set at 5.0 nm. ^{1}H NMR spectra were recorded in a Bruker Ultrashield 300 MHz spectrometer. All NMR spectra were obtained in $CDCl_3$ at room temperature and the chemical shifts were reported in δ values (ppm) relative to TMS. The UV-visible spectra were recorded on a Shimadzu UV-vis-1800 spectrophotometer. The metal salt solutions (10^{-3} M) were prepared in phosphate buffer solution (PBS) at pH 7.0.

Synthesis of Sensor (L)

One m mol (0.112 g) of l-alanine and 1 m mol (0.90 mL) of salicylaldehyde were taken in a 1:5 (v/v) mixture of water and methanol (30 mL) in a round bottom flask. The mixture was stirred for 24 h to get an oily product. The solvent was evaporated in rota evaporator to obtain a dark greenish coloured product which was recrystallized from methanol (mp = 110 °C, yield = 70 %) (Scheme 1).

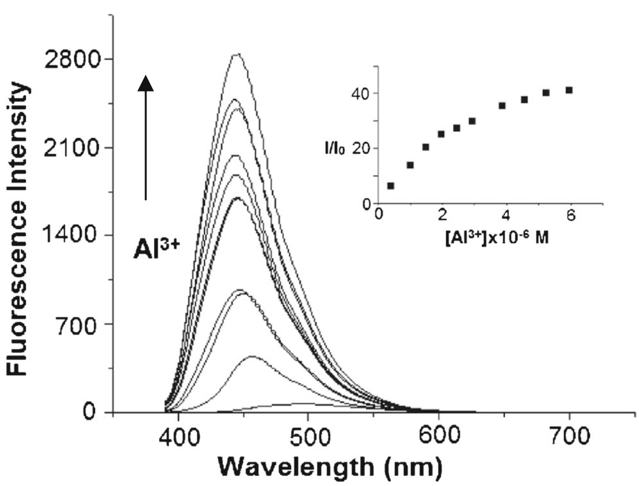

Fig. 1 Fluorescence spectral changes of **L** (5×10^{-6} M) at different added concentration of Al^{3+} ion in 1:1 (*v*/*v*) $CH_3OH{:}H_2O$ (pH = 7.0)

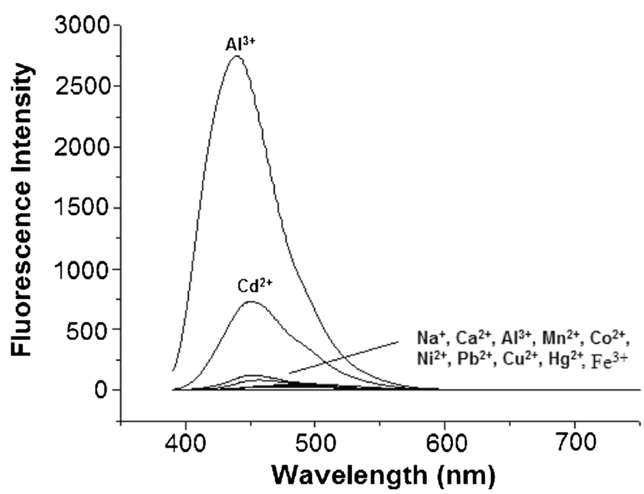

Fig. 2 Fluorescence spectra of **L** (5×10^{-6} M) in 1:1 (*v*/*v*) $CH_3OH{:}H_2O$ (pH = 7.0) in presence of one equivalent amount of Al^{3+} ion and metal ions - Na^{+}, K^{+}, Ca^{2+}, Mn^{2+}, Co^{2+}, Ni^{2+}, Cu^{2+}, Pb^{2+}, Cd^{2+}, Hg^{2+} and Fe^{3+}

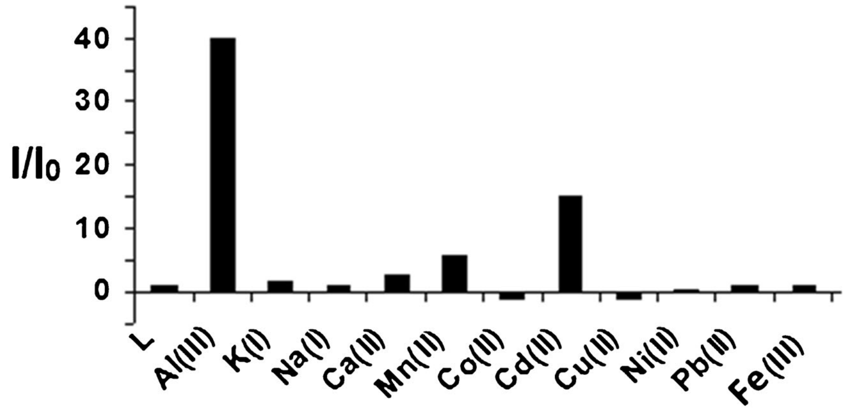

Fig. 3 Bar diagram comparing the I/I_0 values of **L** (5×10^{-6} M) in 1:1 (*v*/*v*) CH_3OH:H_2O (pH = 7.0) upon interaction with Al^{3+} and metal ions - Na^+, K^+, Ca^{2+}, Mn^{2+}, Co^{2+}, Ni^{2+}, Cu^{2+}, Pb^{2+}, Cd^{2+}, Hg^{2+}, and Fe^{3+}

FT-IR spectrum (KBr): 3400 cm^{-1} due to $\nu_{O\text{-}H}$; 1635 cm^{-1} due to $\nu_{C=N}$; 1645 cm^{-1} due to $\nu_{C=O}$; 1315 cm^{-1} due to $\nu_{C\text{-}N}$; 761 cm^{-1} due to $\delta_{=C\text{-}H}$. **^{1}HNMR** ($CDCl_3$, δ in ppm, TMS): 11.03 (COOH); 8.32 (=N-CH); 7.45, 7.11, 6.86, 6.73 (phenyl ring H); 4.94 (−OH); 4.50 (N-CH); 1.70 ($-CH_3$).

Computational Details

The ground state geometrical minima of the ligand was optimized at B3LYP/6-311++G(d,p) [24–27] and was confirmed by the absence of any imaginary frequency. Further, time dependent DFT (TDDFT) calculations were performed on the optimized structures of the **L**:Al^{3+} complex to assign the observed electronic transitions in the UV–Visible spectra [28–30], which is implemented in Gaussian09 [31]. The TDDFT calculations were carried out at the same level of theory in gas phase using N states =40.

Results and Discussion

Fluorescence Detection of Al^{3+} by L

L (5×10^{-6} M) in 1:1 (*v*/*v*) CH_3OH:H_2O showed moderate fluorescence with intensity *ca.* 70 when excited with 380 nm photon. The fluorescence emission was observed in 390 nm to 600 nm range with λ_{max} at 495 nm. Fluorescence spectra of **L** were recorded at different added concentration of Al^{3+}. The fluorescence intensity was found to increase gradually with Al^{3+} accompanied by a blue shift in λ_{max} to 460 nm (Fig. 1). The enhancement in fluorescence intensity ceases when **L**:Al^{3+} concentration ratio became 1:1. The final fluorescence intensity was *ca.* 40 times to that of the initial one. Figure 1, Inset shows the plot of I/I_0 as a function of Al^{3+} concentration where I_0 and I are the fluorescence intensities of **L** in absence and presence of Al^{3+} respectively.

Similar fluorescence titrations were performed for **L** (5×10^{-6} M) in 1:1 (*v*/*v*) CH_3OH:H_2O for metal ions - Na^+, K^+, Ca^{2+}, Mn^{2+}, Co^{2+}, Ni^{2+}, Cu^{2+}, Pb^{2+}, Cd^{2+}, Hg^{2+} and Fe^{3+}. Figure 2 shows the effect of these metal ions and Al^{3+} ion on fluorescence spectra of **L**. From the figure it can be seen that the effect of Al^{3+} ion on the fluorescence intensity of **L** is quite distinctive over the rest of metal ions. The effect of different metal ions on I/I_0 values of **L** has been compared by the bar diagram shown in Fig. 3. Where, I and I_0 are the fluorescence intensities of **L** in presence and absence of a metal ion respectively. Fluorescence quenching was observed for Co^{2+} and Cu^{2+} while a moderate fluorescence enhancement of *ca.* 15 times was observed for Cd^{2+}. No significant enhancement or quenching in fluorescence intensity of **L** was observed for interaction with the rest of the metal ions. Figures 2 and 3 clearly prove that **L** acts as a fluorescent sensor for Al^{3+} is over metal ions - Na^+, K^+, Ca^{2+}, Mn^{2+}, Co^{2+}, Ni^{2+}, Cu^{2+}, Pb^{2+}, Cd^{2+}, Hg^{2+} and Fe^{3+}.

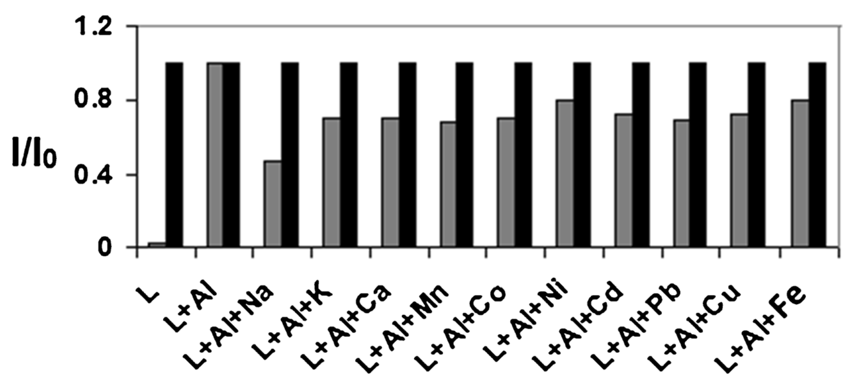

Fig. 4 Bar diagram comparing the I/I_0 values of **L** + Al^{3+} (*black bars*) and **L**+ Al^{3+}+M^{n+} (gray bars) to show the selectivity of **L** towards Al^{3+} over metal ions- Na^+, K^+, Ca^{2+}, Mn^{2+}, Co^{2+}, Ni^{2+}, Cu^{2+}, Pb^{2+}, Cd^{2+}, Hg^{2+} and Fe^{3+}

In order to prove the selectivity of **L** towards Al^{3+} in presence of other metal ions, fluorescence spectra were recorded for **L** in presence of one equivalent each of Al^{3+} and another metal ion viz. Na^+, K^+, Ca^{2+}, Mn^{2+}, Co^{2+}, Ni^{2+}, Cu^{2+}, Pb^{2+}, Cd^{2+}, Hg^{2+} and Fe^{3+}. The I/I_0 values have been compared with I/I_0 value of **L** in presence of one equivalent of Al^{3+} ion only (no other metal ion) through bar diagram (Fig. 4). Here, I_0 is the fluorescence intensity of **L** while I is the fluorescence intensity of **L** in presence of one equivalent of Al^{3+} or Al^{3+} and one equivalent of a metal ion. Comparable heights of the bars corresponding to **L** with Al^{3+} and **L** with Al^{3+} and another metal ion were observed. This confirms that the interaction between **L** and Al^{3+} is stronger than that between **L** and other metal ions. However in presence of Na^+ ion the selectivity of **L** towards Al^{3+} was found to be a little less.

The binding constant and stoichiometry of binding was determined from fluorescence data as reported [17]. For this purpose, $\log[(I_0\text{-}I)/(I\text{-}I_{max})]$ was plotted against $\log[Al^{3+}]$, where I_0 is the fluorescence intensity of **L**, I is the fluorescence intensity of **L** at a given added concentration of Al^{3+} and I_{max} is the fluorescence intensity of I_{max} at one equivalent concentration of Al^{3+}. The plot of $\log[(I_0\text{-}I)/(I\text{-}I_{max})]$ versus $\log[Al^{3+}]$ was linear (Fig. 5). The slope of the plot is 1.19 which implies that the binding interaction between **L** and Al^{3+} is 1:1. The binding constant was calculated as $10^{4.5}$.

The binding stoichiometry and the binding constant, obtained from fluorescence data, between **L** and Al^{3+} were confirmed by UV/visible spectroscopy. UV/visible spectra were recorded for **L** in 1:1 (*v*/*v*) $CH_3OH:H_2O$ with peaks observed at λ_{max} 260 nm, 340 nm and 420 nm. Effect of Al^{3+} on the UV/Visible spectra of **L** has been shown in Fig. 6. With the addition of Al^{3+} the peak at 420 nm gradually disappeared, the peak at 340 nm was shifted to 350 nm with little increase in absorbance and absorbance of the peak at 260 nm decreased a little with no change in peak position. The plot of $\log[(A_0\text{-}A)/(A\text{-}A_{max})]$ against $\log[Al^{3+}]$ was found to be linear (Fig. 6, inset) where A_0 is the absorbance of **L**, A is the absorbance of **L** at a given added concentration of Al^{3+} and A_{max} is the absorbance at one equivalent concentration of Al^{3+}. The binding stoichiometry between **L** and Al^{3+}, which is given by the slope of the plot, was 1:1 with binding constant $10^{4.2,}$ which is given by the intercept at abscissa. These values are in good agreement with those obtained from fluorescence data. The detection limit of **L** towards Al^{3+} was calculated from the plot of normalised fluorescence intensity versus $\log[Al^{3+}]$, as reported [32] and found to be ca. 10^{-6} M.

The enhancement in fluorescence intensity of **L** on interaction with Al^{3+} could be explained on the basis of photoinduced electron transfer (PET) process. The electron density on the lone pairs of N and the pair of O atoms in the sensor gets transferred to the LUMO of the fluorophore part which is comprised of the phenyl ring and the immine bond. This causes the low fluorescence of **L** in unbound to Al^{3+} form. When Al^{3+} binds to **L** through the N and the O lone pairs, the PET process stops and enhancement in fluorescence intensity was observed.

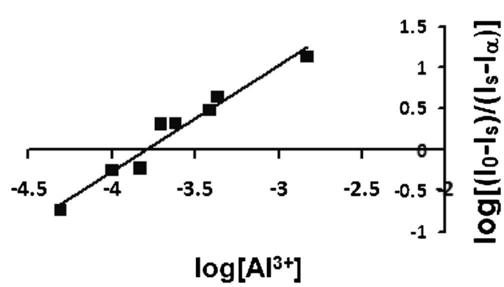

Fig. 5 Plot of $\log[(I_0\text{-}I_s)/(I_s\text{-}I_\alpha)]$ versus $\log[Al^{3+}]$ for **L** in 1:1 (*v*/*v*) $CH_3OH:H_2O$ (pH = 7.0). The solpe = 1.21 indicates 1:1 interaction between **L** and Al^{3+} ion, binding constant calculated as $10^{4.5}$

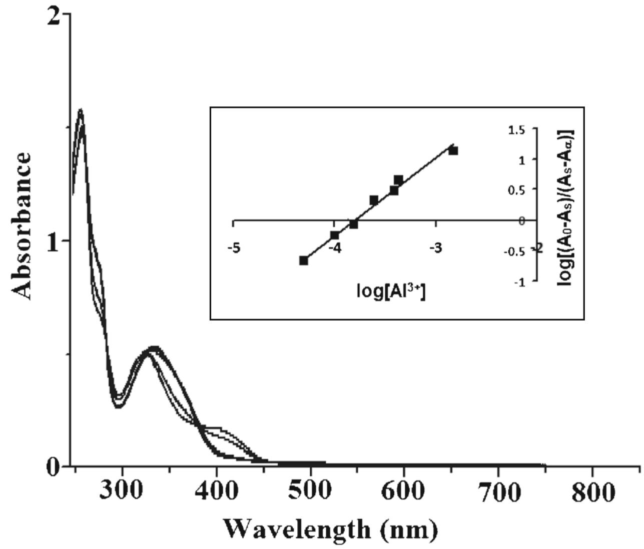

Fig. 6 Change in UV/Visible spectra of **L** (10^{-3} M) in 1:1 (*v*/*v*) $CH_3OH:H_2O$ (pH 7.0) with the addition of Al^{3+}. *Inset* Plot of $\log[(A_0\text{-}A_s)/(A_s\text{-}A_\alpha)]$ versus $\log[Al^{3+}]$

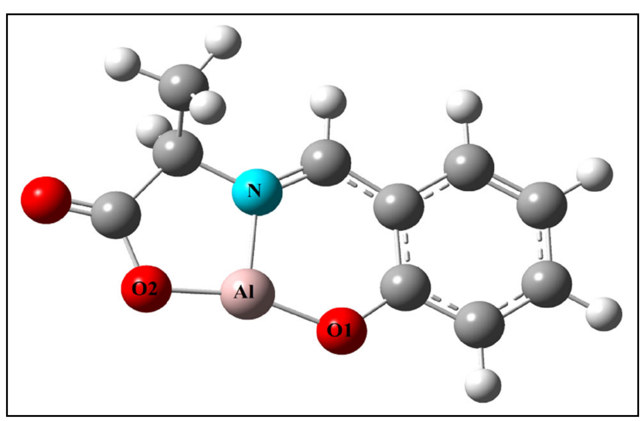

Fig. 7 Optimized structure of the **L**:Al^{3+} complex obtained at B3LYP/6–311++G(d,p) level of theory

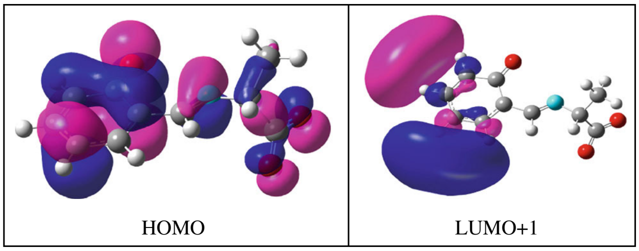

Fig. 8 Shapes of HOMO and LUMO + 1 orbitals of **L**

DFT and TDDFT Calculations

Fluorescence data have confirmed that **L** and Al^{3+} interact in 1:1 ratio. To ascertain the structure of **L**:Al^{3+} complex, the DFT calculation was performed. DFT optimised structure, as shown in Fig. 7, revealed that one Al^{3+} ion binds to one **L** through three binding sites - phenolic O, acetate O and immine N. The Al^{3+} to these binding sites bond lengths were found to be 1.70 Å, 1.71 Å and 1.83 Å respectively. Further, this bonding pattern has been proved by matching electronic spectra obtained from TDDFT calculation with the experimental one.

Experimental UV-visible spectra showed that the ligand possesses a peak at 410 nm which matches with the TDDFT results. The TDDFT calculations also confirmed the presence of the peak to be due to HOMO→LUMO + 1 transition. The shape of the MO associated with this transition is shown in Fig. 8. From the shape of the HOMO it is observed that once the Al^{3+} ion binds **L**, the electron density which was associated with acetate O sites would no longer be available for electronic transition (at 410 nm), and thus quenching the 410 nm peak.

Conclusion

The condensation product of L-alanine and salicylaldehyde acts as fluorescent sensor for Al^{3+} ion by "off-on" mode (detection limit, 10^{-6} M). The sensor was selective for Al^{3+} ion over metal ions - Na^{+}, K^{+}, Ca^{2+}, Mn^{2+}, Co^{2+}, Ni^{2+}, Cu^{2+}, Pb^{2+}, Cd^{2+}, Hg^{2+} and Fe^{3+}. A 1:1 interaction between the sensor and Al^{3+} ion with binding constant $10^{4.5}$ was proved from fluorescence as well as UV/visible spectral data. DFT and TDDFT calculations confirmed the 1:1 interaction between Al^{3+} and the sensor.

Acknowledgments DST, New Delhi and UGC, New Delhi are thanked for financial support to the department through FIST-II and SAP respectively.

References

1. Goswami S, Paul S, Manna A (2013) Selective "naked eye" detection of Al(III) and PPi in aqueous media on a rhodamine–isatin hybrid moiety. RSC Adv 3:10639–10643
2. Verstraeten SV, Aimo L, Oteiza PI (2008) Aluminium and lead: molecular mechanisms of brain toxicity. Arch Toxicol 82:789–802
3. Wang B, Xing W, Zhao Y, Deng X (2010) Effects of chronic aluminum exposure on memory through multiple signal transduction pathways. Environ Toxicol Pharmacol 29:308–313
4. Delhaize E, Ryan PR (1995) Aluminum toxicity and tolerance in plants. Plant Physiol 107:315–321
5. Han T, Feng X, Tong B, Barcelo J, Poschenrieder C (2002) Environ Exp Bot 48:75–92
6. Shi L, Chen L, Zhi J, Dong T (2012) A novel "turn-on" fluorescent chemosensor for the selective detection ofAl^{3+} based on aggregation-induced emission. Chem Commun 48: 416–418
7. Sang H, Liang P, Du D (2008) Determination of trace aluminum in biological and water samples by cloud point extraction preconcentration and graphite furnace atomic absorption spectrometry detection. J Hazard Mater 154:1127–11326
8. Djane SJ, Gra M, Korn C (2000) A separation method to overcome the interference of aluminium on zinc determination by inductively coupled plasma atomic emission spectroscopy. Spectrochim Acta B 55:389–394
9. Abbasi S, Farmany A (2009) Food Chem 116:1019–1023
10. Gupta VK, Jain AK, Maheshwari G (2007) Aluminum(III) selective potentiometric sensor based on morin in poly(vinyl chloride) matrix. Talanta 72:1469–1473
11. Fan L, X-hui J, Wang B-d, Yang Z-y (2014) 4-(8 -hydroxyquinolin-7 -yl)methyleneimino-1-phenyl-2,3- dimethyl-5-pyzole as a fluorescent chemosensor for aluminum ion in acid aqueous medium. Sensors Actuators B 205:249–254
12. J-can Q, T-rong L, Wang B-d, Yang Z-y, Fan L (2014) Fluorescent sensor for selective detection of Al^{3+} based on quinoline–coumarin conjugate. Spectrochim Acta A Mole Biomole Spectro 133:38–43
13. Malkondu S (2014) A highly selective and sensitive perylenebisimide-based fluorescent PET sensor for Al^{3+} determination in MeCN. Tetrahedron 70:5580–5584
14. Kima DH, Im YS, Kimb H, Kima C (2014) Solvent-dependent selective fluorescence sensing of Al^{3+} and Zn^{2+} using a single Schiff base. Inorg Chem Commun 45:15–19
15. Li T, Fang R, Wang B, Shao Y, Liu J, Zhang S, Yang Z (2014) A simple coumarin as a turn-on fluorescence sensor for Al(III) ions. Dalton Trans 43:2741–2743
16. Patil R, Moirangthem A, Butcher R, Singh N, Basu A, Tayade K, Fegade U, Hundiwale D, Kuwar A (2014) Al^{3+} selective colorimetric and fluorescent red shifting chemosensor: application in living cell imaging. Dalton Trans 43:2895–2899
17. Dutta K, Deka R C, Das D K (2014) A new fluorescent and electrochemical Zn^{2+} ion sensor based on Schiff base derived from benzil and L-tryptophan. Spectrochim Acta A Mol Biomol Spectrosc 124:124–129
18. Dutta K, Deka RC, Das DK (2013) A new on-fluorescent probe for manganese (II) ion. J Fluoresc 23:1173–1178
19. Kumar J, Bhattacharyya P, Das DK (2015) New duel fluorescent "on–off" and colorimetric sensor for copper(II): copper(II) binds through N coordination and pi cation interaction to sensor. Spectrochim Acta A Mol Biomol Spectrosc 138:99–104
20. Kumar J, Sarma MJ, Phukan P, Das DK (2015) A new simple Schiff base fluorescence "on" sensor for Al^{3+} and its living cell imaging. Dalton Trans 44:4576–45881
21. Parr RG (1995) Density-functional theory of the electronic structure of molecules. Annu Rev Phys Chem 46:701–728
22. Koch W, Holthausen MC (2001) A chemist's guide to density functional theory, 2nd edn. Wiley-VCH, New York
23. Fiolhais C, Nogueira F, Marques M (2003) A primer in density functional theory. Springer-Verlag Berlin, Heidelberg

24. Mc Lean AD, Chandler GS (1980) Contracted Gaussian basis sets for molecular calculations. I. Second row atoms, Z = 11–18. J Chem Phys 72:5639–5648
25. Raghavachari K, Binkley JS, Seeger R, Pople JA (1980) Self-consistent molecular orbital methods. XX. A basis set for correlated wave functions. J Chem Phys 72:650
26. Becke AD (1993) Density-functional thermochemistry. III The Role of Exact Exchange J Chem Phys 98:5648–5652
27. Lee C, Yang W, Parr RG (1988) Development of the colle-salvetti correlation-energy formula into a functional of the electron density. Phys Rev B 37:785–789
28. Stratmann RE, Scuseria GE, Frisch MJ (1998) An efficient implementation of time-dependent density-functional theory for the calculation of excitation energies of large molecules. J Chem Phys 109:8218–8224
29. Bauernschmitt R, Ahlrichs R (1996) Treatment of electronic excitations within the adiabatic approximation of time dependent density functional theory. Chem Phys Lett 256:454
30. Casida ME, Jamorski C, Casida KC, Salahub DR (1998) Molecular excitation energies to high-lying bound states from time-dependent density-functional response theory: characterization and correction of the time-dependent local density approximation ionization threshold. J Chem Phys 108:4439–4449
31. Gaussian 09, Revision B.01, Frisch et al. Gaussian, Inc., Wallingford CT 2010
32. Shortreed M, Kopelman R, Kuhn M, Hoyland B (1996) Fluorescent fiber-optic calcium sensor for physiological measurements. Anal Chem 68:1414–1418